SMC-TR-98-39

AEROSPACE REPORT NO.
TR-98(8570)-5

# Storm/Substorm Signatures in the Outer Radiation Belt

15 January 1999

Prepared by

A. KORTH, R. H. W. FRIEDEL, and C. MOUIKIS
Max Planck-Institut für Aeronomie
Lindau, Germany

and

J. F. FENNELL
Space and Environment Technology Center
Technology Operations

Prepared for

Engineering and Technology Group

19990209 142

**THE AEROSPACE
CORPORATION**
El Segundo, California

DTIC QUALITY INSPECTED 2

Peter Bissegger
SMC/AXES

# REPORT DOCUMENTATION PAGE

Public reporting burden for this collection of information is estimated to average 1 hour per response, including the time for reviewing instructions, searching existing data sources, gathering and maintaining the data needed, and completing and reviewing the collection of information. Send comments regarding this burden estimate or any other aspect of this collection of information, including suggestions for reducing this burden to Washington Headquarters Services, Directorate for Information Operations and Reports, 1215 Jefferson Davis Highway, Suite 1204, Arlington, VA 22202-4302, and to the Office of Management and Budget, Paperwork Reduction Project (0704-0188), Washington, DC 20503.

| 1. AGENCY USE ONLY (Leave blank) | 2. REPORT DATE<br>15 January 1999 | 3. REPORT TYPE AND DATES COVERED |
|---|---|---|

**4. TITLE AND SUBTITLE**

Storm/Substorm Signatures in the Outer Radiation Belt

**6. AUTHOR(S)**

Korth, A., Friedel, R. H. W., and Mouikis, C., Max-Planck-Institut für Aeronomie; Fennell, J. F., The Aerospace Corporation

**5. FUNDING NUMBERS**

F04701-93-C-0094

**7. PERFORMING ORGANIZATION NAME(S) AND ADDRESS(ES)**

The Aerospace Corporation
Technology Operations
El Segundo, CA 90245-4691

**8. PERFORMING ORGANIZATION REPORT NUMBER**

TR-98(8570)-5

**9. SPONSORING/MONITORING AGENCY NAME(S) AND ADDRESS(ES)**

Space and Missile Systems Center
Air Force Materiel Command
2430 E. El Segundo Blvd.
Los Angeles Air Force Base, CA 90245

**10. SPONSORING/MONITORING AGENCY REPORT NUMBER**

SMC-TR-98-39

**11. SUPPLEMENTARY NOTES**

**12a. DISTRIBUTION/AVAILABILITY STATEMENT**

Approved for public release; distribution unlimited

**12b. DISTRIBUTION CODE**

**13. ABSTRACT** (Maximum 200 words)

The response of the ring current region is compared for periods of storm and substorm activity, with an attempt to isolate the contributions of both processes. We investigate CREES particle data in an overview format that allows the display of long-term variations of the outer radiation belt. We compare the evolution of the ring current population to indicators of storm ($Dst$) and substorm ($AE$) activity and examine compositional changes. Substorm activity leads to the intensification of the ring current at higher L ($L \sim 6$) and lower ring current energies compared to storms ($L \sim 4$). The $O^+/H^+$ ratio during substorms remains low, near 10%, but is much enhanced during storms (can exceed 100%). We conclude that repeated substorms with an $AE \sim 900$ nT lead to a $\Delta Dst$ of $\sim 30$ nT, but do *not* contribute to $Dst$ during storm main phase as substorm injections do not form a symmetric ring current during such disturbed times.

**14. SUBJECT TERMS**

CRRES
Magnetosphere
Radiation Belt
Substorms

**15. NUMBER OF PAGES**

10

**16. PRICE CODE**

| 17. SECURITY CLASSIFICATION OF REPORT<br>Unclassified | 18. SECURITY CLASSIFICATION OF THIS PAGE<br>Unclassified | 19. SECURITY CLASSIFICATION OF ABSTRACT<br>Unclassified | 20. LIMITATION OF ABSTRACT |
|---|---|---|---|

# Storm/substorm signatures in the outer radiation belt

A. Korth, R. H. W. Friedel[1] and C. Mouikis

Max-Planck-Institut für Aeronomie, Lindau, Germany

J. F. Fennell

The Aerospace Corporation, El Segundo, USA

**Abstract.** The response of the ring current region is compared for periods of storm and substorm activity, with an attempt to isolate the contributions of both processes. We investigate CRRES particle data in an overview format that allows the display of long-term variations of the outer radiation belt. We compare the evolution of the ring current population to indicators of storm ($Dst$) and substorm ($AE$) activity and examine compositional changes. Substorm activity leads to the intensification of the ring current at higher L ($L \sim 6$) and lower ring current energies compared to storms ($L \sim 4$). The $O^+/H^+$ ratio during substorms remains low, near 10%, but is much enhanced during storms (can exceed 100%). We conclude that repeated substorms with an $AE \sim 900$ nT lead to a $\Delta Dst$ of $\sim 30$ nT, but do *not* contribute to $Dst$ during storm main phase as substorm injections do not form a symmetric ring current during such disturbed times.

## Introduction

The role of storms in the filling of the radiation belts and the ring current region has been well established [*Lui et al.*, 1987; *Lyons and Williams*, 1975]. The exact role that substorms can play in this scenario is still a matter of debate.

Substorms generally occur more frequently during the active phase of a storm, and can substantially modify the recovery behavior of storms *Gonzalez et al.* [1994], leading to a much slower recovery in the presence of multiple substorms. It has been difficult up to now to differentiate between storm only changes in the ring current ($Dst$) and the substorm contribution to these changes. *McPherron* [1997] in his statistical study of the role of substorms during magnetic storms concludes that the effect of particles injected during substorm expansion phase is undetectable in the pressure corrected $Dst$ index. On the other hand, *Gonzalez et al.* [1994] shows clearly how continuous substorm activity in the recovery phase can keep $Dst$ depressed for days after a storm. Simulation work with the Magnetospheric Specification and Forecast Model *Wolf et al.* [1997] has addressed this question as well. They concluded that potential convection electric fields during the storm main phase play a far more important role in ring current injection than do substorm-associated induction fields. They also show that when the magnetosphere is highly compressed $> 50$ keV ions are shadowed by the magnetosphere. Substorm injections during such times are thus unlikely to yield symmetric ring current contributions and do not have long lifetimes.

To compliment the statistical and modeling work mentioned above We investigate here particle populations as measured in the inner magnetosphere. We extend here on the work of *Korth and Friedel* [1997] which investigated storm-time dynamics to include substorm-only times as well. We present electron and ion composition measurements over the whole outer region for two separate events - one a classic storm and one a series of substorms which in their $Dst$ signatures would be classed as a "small storm" [*Gonzalez et al.*, 1994]. By separating out the two classes of events, which normally occur as a superposition of one another, we can determine their individual responses. We further include ion composition measurements, in order to determine the contribution of individual species to the ring current density.

## Mission and Instrumentation

This study uses particle measurements on the Combined Release and Radiation Effects Satellite (CRRES), which had an elliptical, $18.1^o$ inclination orbit, and covered the regions up to $L = 8$, giving an $L$-

---

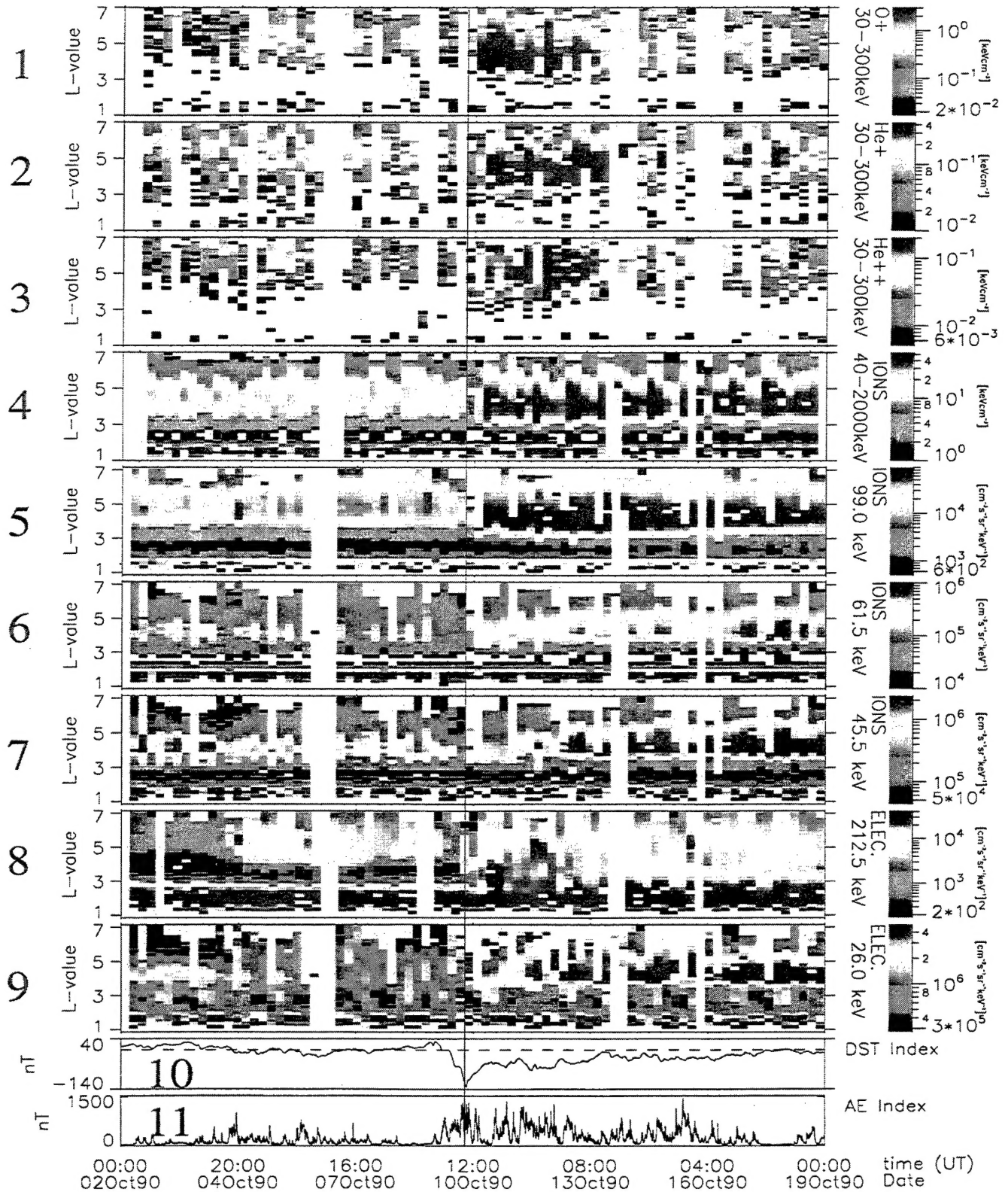[1]Now at NIS-2, Los Alamos National Laboratory, Los Alamos, New Mexico, USA

**Plate 1.** Data for the intense storm 9/10 October 1990. See text for details.

The color version of this plate is available from J. F. Fennell.

profile twice an orbit, at magnetic latitudes mostly within $20^o$ of the magnetic equator.

On CRRES, the Medium Electrons B spectrometer (MEB, *Korth et al.* [1992]) covers electrons from 21 keV to 285 keV and total ions (no composition) from 37 keV to 3.2 MeV. The Medium Electrons A spectrometer (MEA, *Vampola et al.* [1992]) covers electrons from 143 keV to 1.58 MeV. The Magnetospheric Ion Composition Spectrometer (MICS, *Wilken et al.* [1992]) measures the mass, energy, and the charge of particles with energies of 1–430 keV/charge.

## Observations

The data presented in this paper are L-sorted plots versus time of the type used by *Friedel and Korth* [1995]; *Korth and Friedel* [1997]. For each half-orbit (4:55 hours) the data binned in 0.2 $L$ which is one vertical stripe in the plots. $L$-values are from the Olson-Pfitzer 1977 quiet model. Magnetic latitude dependence is corrected in the MEB data set [*Friedel and Korth*, 1995].

In Plates 1,2 the panels are numbered in red from the top, $1 \rightarrow 11$.

Panels 10, 11 show $Dst$ as a measure of the ring current, and the $AE$ as a measure of substorm activity.

Panels 1–9 show the particle populations inside the magnetosphere:

Panels 5–7 displays three ion flux channels with peak energies of 45.5, 61.5, and 99 keV and panels 8 and 9 two electron flux channels with peak energies of 26 and 212.5 keV. This energy range represents the peak of the ring current density (30-300 keV).

Panel 4 displays the energy density of all ions (mostly $H^+$) in the ring current, as determined from the MEB instrument.

Panels 1 to 3 show the energy density of heavier ions ($O^+$, $He^+$, $He^{++}$).

### Classic Storm (9/10 October 1990)

An isolated magnetic storm ($Dst = -133$ nT) is shown in Plate 1 over a time period of 17 days. The ($B_z$, $\Delta T$) trigger of -8.7 nT for about 10 hours indicates an intense storm [*Gonzalez et al.*, 1994]. Northward turning of $B_z$ (solid line) initiates the recovery phase.

Comparing P1anels 10 and 11 shows that the normal exponential recovery of the storm in $Dst$ is delayed at the time of onset of a series of substorms. The

particles injected by these substorms are not clearly seen except at high $L$ in Panel 9.

We identify the maximum of the outer radiation belt in this energy range (panel 4) as being roughly the "position" of the ring current. The prestorm maximum is between L=3.5–5.5 for these energies. With the beginning of the recovery phase the ring current intensifies (electrons and ions) and the maximum is displaced earthward by about half an Earth radius. The slot region narrows and widens again later.

$He^{++}$ (alpha particles) have direct access during the storm and decay due to charge exchange to $He^+$ and diffuse radially inward during the storm recovery phase, and thus reach their maximum intensity $\sim 5$ hours after recovery onset. The maximum energy density of $He^{++}$ is between $L = 4.5 \rightarrow 6$, further out than the main ring current density. Due to the low fluxes during this event, and the delayed appearance these ions do not contribute to the main phase of the storm but may contribute to the delay in recovery. However, the $He^{++}$ flux observed depends very much on the solar wind composition. For the storms investigated so far the energy density ratio of $He^{++}/H^+$ can vary between 2% and 30%.

$O^+$ is of ionospheric source and together with $He^+$ intensifies at storm recovery, and constitutes part of the ring current between $L = 3.5 \rightarrow 5.5$, closer in than the $He^{++}$ contribution. The energy density ratio of $He^+/H^+$ and $O^+/H^+$ is 0.02 and 0.22, respectively. The ratio increases normally with increasing $Dst$ and for $O^+/H^+$ in particular can reach 50% [*Daglis*, 1997]. $O^+$ can thus be a major ring current constituent during storms. $He^+$ is low as it depends on $He^{++}$. The contribution of the heavy ions in the ring current decaying on a shorter time scale (a few days) compared within the main ring current. The intensities in Panel 1 to 3 drop off quickly after 3 days, at which time $Dst$ also shows an accelerated recovery.

### Substorms Series (6–16 February 1991)

Plate 2 shows a ten days period during which we observe continuous substorm activity. A solid line indicates the onset of this activity and the beginning of a decrease in $Dst$ to a minimum of -34 nT. Each major peak in $AE$ is associated with a decrease in $Dst$. During this time the $B_z$-component of the IMF (not shown) exhibits small-amplitude fluctuations with negative excursions between 1.5 and 4.5 nT for durations of up to four hours.

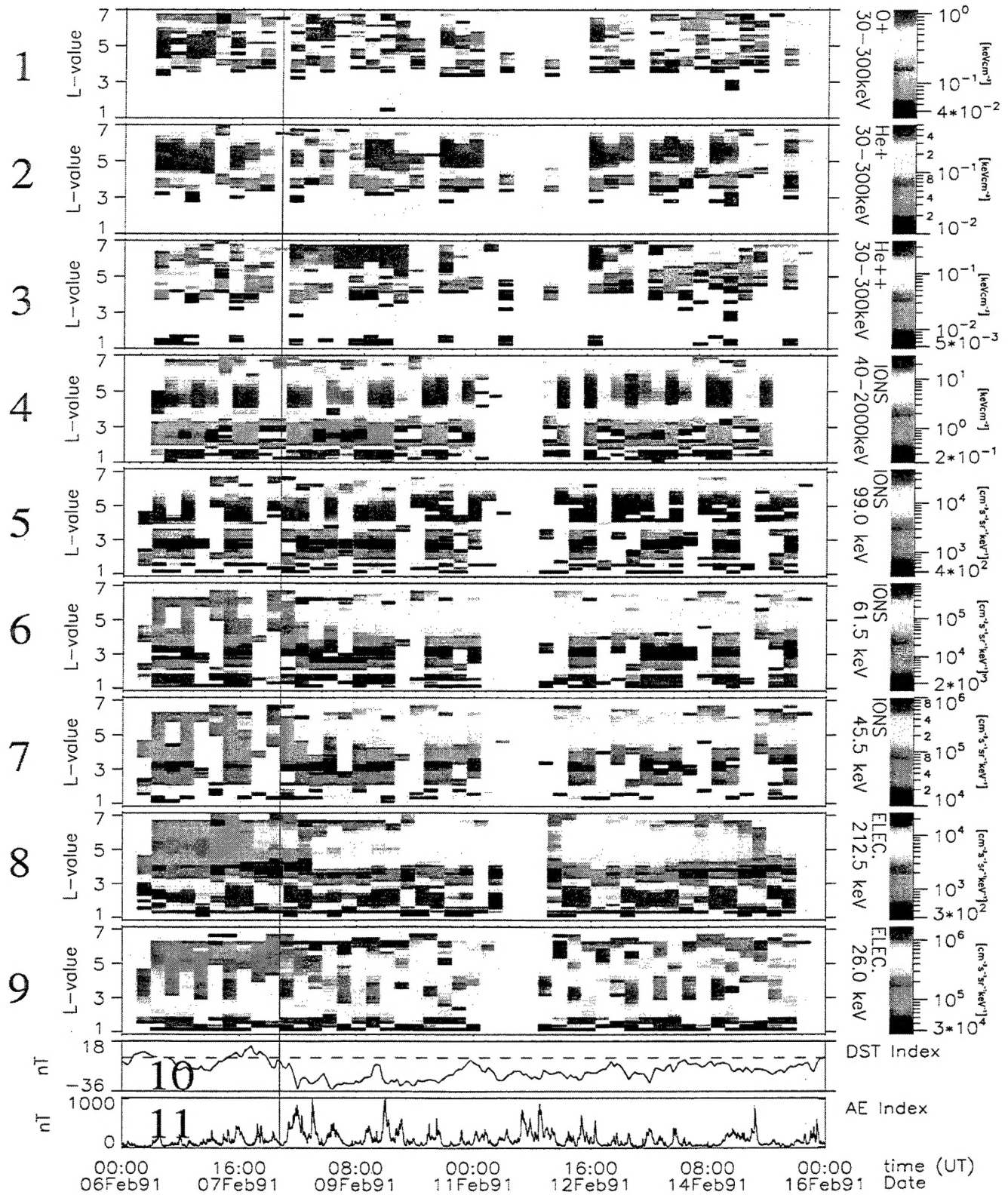The $AE$ index fluctuations are reflected by the in-

**Plate 2.** Data for the series of substorms 6-16 February 1991. See text for details.
The color version of this plate is available from J. F. Fennell.

jections (substorms) of low energy electrons with peak energies of 26 keV (panel 9) at L-values between 5 and 7. These injected particles diffuse radially inward and lead to a symmetric ring current. An intensification of the ring current is also observed in the 212.5 keV electron channel. In the ion channels ring current intensification is seen only for energies up to 85 keV. The 99 keV ion channel (panel 5) indicates no flux intensification which means that the intensity of the quiet ring current is not changing evidently during the ten days period. The maximum of the quiet time ring current is about at $L = 5$, whereas the maximum of the injected particles are further out at $L = 5.5$.

The composition response shows marked differences compared with the storm case. $O^+$ shows short-lived responses to individual $AE$ events, which occur further out near $L = 6$. $He^{++}$ shows a build up also near $L = 6$, showing solar wind plasma access to the inner magnetosphere during substorms. $He^{++}$ builds up slowly and has a longer lifetime than $O^+$, forming a more continuous belt at $L = 6$. The delayed response of $He^+$ is consistent with the charge-exchange dependence on $He^{++}$, "outliving" $He^{++}$ by the same delay of about one day.

$He^{++}$ reaches a maximum $He^{++}/H^+$ energy density ratio levels of 2%, and thus has a negligible effect on $Dst$. The energy density ratio for $O^+/H^+$ is 9%, and that for $He^+/H^+$ 6% . Thus none of the heavier ions are major contributors to substorm related changes in $Dst$.

## Summary

CRRES particle data in a $L$ versus time format allows tracking of the radiation belt particle population during storms and substorms.

During storm the observable effect of substorms seems to be limited to delaying the recovery phase, while the data shows no clear indication of substorm injections down to the main body of the ring current during the storm onset phase. The main body of the ring current moves inwards from it's normal position of L=4.5–5 and intensifies, which correlated well with the behavior of $Dst$. Thus our data does not support the Chapman's original hypothesis storm = $\Sigma$ substorms.

The observed dramatic increase in the $O^+/H^+$ ratio during storms is also a storm-only effect, as it is not observed for substorms on their own. We have shown that the compositional changes associated with substorms do not have an effect on $Dst$ and can be ignored.

For substorms the ring current intensification is less and only at lower energies, and occurs further out at L-values between 5 and 7. All these factors explain the moderate effect on $Dst$. A rough correlation of $AE$ to $Dst$ shows that a series of $AE \sim 800\text{-}1000$ nT events leads to a change in $Dst$ cf $\sim 30$ nT. Applying this rough relation to the 9/10 Oct storm, which showed 1400nT $AE$ substorms *during* the storm main phase, this would lead to a substorm contribution to the minimum $Dst$ observed of $\sim 45$nT or 30%. However, this should be detectable by a fairly strong substorm-related increase in the particle populations at higher L, which is not observed.

A possible explanation of this is that the substorm injections during the main phase of a storm occur when the magnetosphere is much distorted, so that injections at higher $L$ do not complete a full drift and never form into a symmetrical ring current, whereas substorm injections do create a symmetrical rung current, which forms further out by about one Earth radius compared to the normal ring current. This result supports the findings of *McPherron* [1997] who concluded that substorms do not contribute to the storm main phase $Dst$.

We can thus conclude that while substorms may not play a role in ring-current dynamics during the disturbed storm main phase, repeated substorm activity does form a symmetric ring current at higher $L$ thus contributing to $Dst$.

The ion composition measurements showed a strong contribution of $O^+$ during storms. Final storm recovery seems to be more controlled by the recovery of the heavy ions. For substorms ions composition is a minor effect in relation to $Dst$. However we note here the $He^{++}$ observations which show clear solar wind access to the inner magnetosphere. The delayed response indicates that this is not direct access but rather a result of the front-side reconnection / tail convection scenario.

## References

Daglis, I. A., The role of magnetosphe-ionosphere cou-

pling in magnetic storm dynamics, in *Magnetic Storms, Geophysical Monograph 98*, edited by V. T. Tsurutani, W. Gonzalez, Y. Kamide, and J. Arballo, pp. 107–116, AGU, Washington, D.C., 1997.

Friedel, R. H. W., and A. Korth, Long-term observations of kev ion and electron variability in the outer radiation belt from CRRES, *Geophys. Res. Lett.*, *22*, 1853–1856, 1995.

Gonzalez, W., J. Joselyn, Y. Kamide, H. Kroehl, G. Rostoker, B. Tsurutani, and V. Vasyliunas, What is a geomagnetic storm?, *J. Geophys. Res.*, *99*, 5771–5792, 1994.

Korth, A., and R. H. W. Friedel, Dynamics of energetic ions and electrons between $L = 2.5$ and $L = 7$ during magnetic storms, *J. Geophys. Res.*, *102*, 14,113–14,122, 1997.

Korth, A., G. Kremser, B. Wilken, W. Güttler, S. L. Ullaland, and R. Koga, Electron and proton wide-angle spectrometer (EPAS) on the CRRES spacecraft, *J. Spacecr. Rockets*, *29*, 609–614, 1992.

Lui, A. T. Y., R. W. McEntire, and S. M. Krimigis, Evolution of the ring current during two geomagnetic storms, *J. Geophys. Res.*, *92*, 7459–7470, 1987.

Lyons, L., and D. Williams, The storm and poststorm evolution of energetic (35–560 kev) radiation belt electron distributions, *J. Geophys. Res.*, *80*, 3985–3994, 1975.

McPherron, R. L., The role of substorms in the generation of magnetic storms, in *Magnetic Storms, Geophysical Monograph 98*, edited by V. T. Tsurutani, W. Gonzalez, Y. Kamide, and J. Arballo, pp. 131–147, AGU, Washington, D.C., 1997.

Vampola, A. L., J. V. Osborne, and B. M. Johnson, CRRES magnetic electron spectrometer AFGL-701-5A (MEA), *J. Spacecr. Rockets*, *29*, 592–594, 1992.

Wilken, B., W. Weiss, D. Hall, M. Grande, F. Soeraas, and J. F. Fennell, Magnetospheric ion composition spectrometer onboard the CRRES spacecraft, *J. Spacecr. Rockets*, *29*, 585–591, 1992.

Wolf, R. A., J. J. W. Freeman, B. A. Hausman, and R. W. Spiro, Modeling convection effects in magnetic storms, in *Magnetic Storms, Geophysical Monograph 98*, edited by V. T. Tsurutani, W. Gonzalez, Y. Kamide, and J. Arballo, pp. 161–172, AGU, Washington, D.C., 1997.

# TECHNOLOGY OPERATIONS

The Aerospace Corporation functions as an "architect-engineer" for national security programs, specializing in advanced military space systems. The Corporation's Technology Operations supports the effective and timely development and operation of national security systems through scientific research and the application of advanced technology. Vital to the success of the Corporation is the technical staff's wide-ranging expertise and its ability to stay abreast of new technological developments and program support issues associated with rapidly evolving space systems. Contributing capabilities are provided by these individual Technology Centers:

**Electronics Technology Center:** Microelectronics, VLSI reliability, failure analysis, solid-state device physics, compound semiconductors, radiation effects, infrared and CCD detector devices, Micro-Electro-Mechanical Systems (MEMS), and data storage and display technologies; lasers and electro-optics, solid state laser design, micro-optics, optical communications, and fiber optic sensors; atomic frequency standards, applied laser spectroscopy, laser chemistry, atmospheric propagation and beam control, LIDAR/LADAR remote sensing; solar cell and array testing and evaluation, battery electrochemistry, battery testing and evaluation.

**Mechanics and Materials Technology Center:** Evaluation and characterization of new materials: metals, alloys, ceramics, polymers and composites; development and analysis of advanced materials processing and deposition techniques; nondestructive evaluation, component failure analysis and reliability; fracture mechanics and stress corrosion; analysis and evaluation of materials at cryogenic and elevated temperatures; launch vehicle fluid mechanics, heat transfer and flight dynamics; aerothermodynamics; chemical and electric propulsion; environmental chemistry; combustion processes; spacecraft structural mechanics, space environment effects on materials, hardening and vulnerability assessment; contamination, thermal and structural control; lubrication and surface phenomena; microengineering technology and microinstrument development.

**Space and Environment Technology Center:** Magnetospheric, auroral and cosmic ray physics, wave-particle interactions, magnetospheric plasma waves; atmospheric and ionospheric physics, density and composition of the upper atmosphere, remote sensing, hyperspectral imagery; solar physics, infrared astronomy, infrared signature analysis; effects of solar activity, magnetic storms and nuclear explosions on the earth's atmosphere, ionosphere and magnetosphere; effects of electromagnetic and particulate radiations on space systems; component testing, space instrumentation; environmental monitoring, trace detection; atmospheric chemical reactions, atmospheric optics, light scattering, state-specific chemical reactions and radiative signatures of missile plumes, and sensor out-of-field-of-view rejection.